Astrophysical S factor and rate of ^{7}Be$(p,\gamma)^8$B direct capture reaction in a potential model

E. M. Tursunov [*]
Institute of Nuclear Physics, Uzbekistan Academy of Sciences, 100214 Ulugbek, Tashkent, Uzbekistan and National University of Uzbekistan, 100174 Tashkent, Uzbekistan

S. A. Turakulov [†]
Institute of Nuclear Physics, Uzbekistan Academy of Sciences, 100214 Ulugbek, Tashkent, Uzbekistan

A. S. Kadyrov [‡]
Department of Physics and Astronomy and Curtin Institute for Computation, Curtin University, GPO Box U1987, Perth, Western Australia 6845, Australia

L. D. Blokhintsev [§]
Skobeltsyn Institute of Nuclear Physics, Lomonosov Moscow State University, Moscow 119991, Russia

(Received 11 May 2021; accepted 7 October 2021; published 21 October 2021)

The astrophysical ^{7}Be$(p,\gamma)^8$B direct capture process is studied in the framework of a two-body single-channel model with potentials of the Gaussian form. A modified potential is constructed to reproduce the new experimental value of the S-wave-scattering length and the known astrophysical S factor at the Gamow energy, extracted from the solar neutrino flux. The resulting potential is consistent with the theory developed by Baye [Phys. Rev. C **62**, 065803 (2000)] according to which the S-wave scattering length and the astrophysical S factor at zero energy divided by the square of the asymptotic normalization coefficient are related. The obtained results for the astrophysical S factor at intermediate energies are in good agreement with the two data sets of Hammache *et al.* [Phys. Rev. Lett. **86**, 3985 (2001); **80**, 928 (1998)]. Linear extrapolation to zero energy yields $S_{17}(0) \approx 20.51^{+2.02}_{-1.85}$ eV b consistent with the Solar Fusion II estimate. The calculated reaction rates are substantially lower than the results of the NACRE II Collaboration.

DOI: 10.1103/PhysRevC.104.045806

I. INTRODUCTION

The astrophysical capture process ^{7}Be$(p,\gamma)^8$B is the most important nuclear reaction of the pp chain in the Solar Fusion Model and in stellar nucleosynthesis [1–4]. A realistic estimate of the reaction rate of this process is crucial for the solution of the solar neutrino problem. The core temperature of the Sun can be determined through the measurements of the ^{8}B neutrino flux with a precision of about 9% [5]. The rate of the ^{7}Be$(p,\gamma)^8$B reaction is used for modeling this solar neutrino flux.

Many original research papers have been published in addition to reviews [2,3]. Direct measurements face difficulties due to large Coulomb forces at low energies [6–12]. Coulomb dissociation of ^{8}B in the field of a heavy target has been experimentally studied in Refs. [13–17]. However, none of these experimental studies could reach the energies below the solar Gamow window at 0.019 MeV. As a result, the extrapolated value $S_{17}(0)$ of the astrophysical S factor in the "Solar Fusion II" (SF II) workshop,

$$S_{17}(0) = (20.8 \pm 0.7_{\rm expt} \pm 1.4_{\rm theor})\ \text{eV b} \tag{1}$$

has a large uncertainty [3].

From the theory point of view, potential models [18–21], R-matrix parametrization [22], microscopic models [23–25], three-body model [26], *ab initio* calculations [27,28], Skyrme-Hartree-Fock theory [29], and halo effective-field theory [30] have been developed. Results of most theoretical studies for $S_{17}(0)$ belong to the aforementioned uncertainty range of the SF II estimate. In Ref. [31] the reaction ^{10}B$(^7$Be$,^8$B$)^9$Be was used for extracting the asymptotic normalization coefficient (ANC) C for the the virtual transition $p + {^7}$Be $\to$ ^{8}B. Similarly, in Ref. [32] the ANC was extracted from the data of the ^{7}Be$(d,n)^8$B transfer reaction. In Ref. [33] the ANC was derived from the experimental cross section of the ^{13}C$(^7$Li$,^8$Li$)^{12}$C charge-conjugate reaction. As first established in Ref. [34], the astrophysical S factor at low energies is mainly determined by the ANC. The idea is widely used for estimating the astrophysical S factor of capture reactions [31,32,35].

Besides the value of the astrophysical S factor at zero energy, the most important property is the energy dependence

[*]tursune@inp.uz
[†]turakulov@inp.uz
[‡]a.kadyrov@curtin.edu.au
[§]blokh@srd.sinp.msu.ru

of the astrophysical S factor at low energies below the Gamow window. In Ref. [36] the coefficients of the Taylor expansion in terms of energy around zero energy have been found for a given potential. Due to the fact that the largest contribution to the astrophysical S factor of the process at low energies comes from the initial S-wave $p + {}^7$Be scattering state, in Ref. [37] the dependence of $S(0)/C^2$ and $S'(0)/S(0)$ on the S-wave $p + {}^7$Be scattering length have been studied in detail, and important formulas have been derived.

On the other hand, recently in Ref. [38] the most precise experimental values $a_{01} = 17.34^{+1.11}_{-1.33}$ and $a_{02} = -3.18^{+0.55}_{-0.50}$ fm for the s-wave scattering lengths have been obtained in the spin = 1 and spin = 2 channels, respectively. Additionally, a new datum for the astrophysical S factor at the Gamow energy has been extracted from the solar neutrino flux [39] to be

$$S_{17}(19^{+6}_{-5}\ \text{keV}) = (19.0 \pm 1.8)\ \text{eV b}. \tag{2}$$

The aim of the present paper is to estimate S_{17} and corresponding reaction rates in the potential model which reproduces new values of the S-wave scattering length and of S_{17} at the Gamow energy. This paper is based on a single-channel potential model [21]. First we examine and optimize the S-wave potential parameters by fitting to the new value of a_{01}, then we fit the bound ${}^3P_2$ state potential parameters based on the new values of S_{17} at the Gamow energy found in Ref. [39] as described above. Then consistency of the resulting potential with the theory of Ref. [37] is examined.

In Sec. II the theoretical model is described. Section III contains the numerical results. Conclusions are drawn in the last section.

II. THEORETICAL MODEL

A. Wave functions

In the single-channel potential model [40–42], the initial- and final-state wave functions are defined as

$$\Psi^J_{lS} = \frac{u_E^{(lSJ)}(r)}{r}\{Y_l(\hat{r}) \otimes \chi_S(\xi)\}_{JM}, \tag{3}$$

and

$$\Psi^{J_f}_{l_f S'} = \frac{u^{(l_f S' J_f)}(r)}{r}\{Y_{l_f}(\hat{r}) \otimes \chi_{S'}(\xi)\}_{J_f M_f}, \tag{4}$$

respectively. The initial $p - {}^7$Be scattering states in the ${}^3S_1$, ${}^3P_0$, ${}^3P_1$, ${}^3P_2$, ${}^3D_1$, ${}^3D_2$, ${}^3D_3$, and ${}^3F_3$ partial waves are described by the radial wave functions which are solutions of the two-body Schrödinger equation,

$$\left[-\frac{\hbar^2}{2\mu}\left(\frac{d^2}{dr^2} - \frac{l(l+1)}{r^2}\right) + V^{lSJ}(r)\right]u_E^{(lSJ)}(r) = E u_E^{(lSJ)}(r), \tag{5}$$

where μ is the reduced mass of p and ^{7}Be(3/2−), $1/\mu = 1/m_1 + 1/m_2$, and $V^{lSJ}(r)$ is a two-body potential in the partial wave with the orbital angular momentum l, spin S, and total angular momentum J. The wave-function $u^{(l_f S' J_f)}(r)$ of the final ${}^3P_2$ ground state is calculated as a solution of the bound-state Schrödinger equation. The Schrödinger equation is solved using the Numerov algorithm. The cross section, the astrophysical S factor, and the reaction rates are estimated using the accurate wave functions of the initial and final states. The initial scattering wave function is found subject to the asymptotic condition,

$$u_E^{(lSJ)}(r) \underset{r\to\infty}{\rightarrow} \cos\delta_{lSJ}(E)F_l(\eta, kr) + \sin\delta_{lSJ}(E)G_l(\eta, kr), \tag{6}$$

where k is the wave number of the relative motion, η is the Zommerfeld parameter, F_l and G_l are regular and irregular Coulomb functions, respectively, and $\delta_{lSJ}(E)$ is the phase shift in the (l, S, J)th partial wave.

The $p - {}^7$Be two-body potential has the Gaussian form [21],

$$V^{lSJ}(r) = V_0 \exp(-\alpha_0 r^2) + V_c(r), \tag{7}$$

where the Coulomb part is taken in a pointlike potential form [21].

B. Cross sections of the radiative-capture process

The cross section for radiative-capture process can be expressed as [2,21]

$$\sigma(E) = \sum_{J_f \lambda \Omega} \sigma_{J_f \lambda}(\Omega), \tag{8}$$

where $\Omega = E$ or M (electric or magnetic transition), λ is a multiplicity of the transition and J_f is the total angular momentum of the final state. For a particular final state with total angular momentum J_f and multiplicity λ we have [2]

$$\sigma_{J_f\lambda}(\Omega) = \sum_J \frac{(2J_f+1)}{[S_1][S_2]} \frac{32\pi^2(\lambda+1)}{\hbar\lambda([\lambda]!!)^2} k_\gamma^{2\lambda+1} C^2(S) \times \sum_{lS} \frac{1}{k_i^2 v_i} \left|\left\langle \Psi^{J_f}_{l_f S'} \right\| M^\Omega_\lambda \left\| \Psi^J_{lS} \right\rangle\right|^2, \tag{9}$$

where l and l_f are the orbital momenta of the initial and final states, respectively; k_i and v_i are the wave number and speed of the $p - {}^7$Be relative motion in the entrance channel, respectively; S_1 and S_2 are spins of the clusters p and ^{7}Be, $k_\gamma = E_\gamma/\hbar c$ is the wave number of the photon corresponding to energy $E_\gamma = E_{\text{th}} + E$, where E_{th} is the threshold energy for the breakup reaction $\gamma + {}^8\text{B} \rightarrow {}^7\text{Be} + p$. Constant $C^2(S)$ is a spectroscopic factor [2]. Within the potential approach where the bound and scattering properties (energies, phase shifts, and scattering length) are reproduced, a value of the spectroscopic factor must be taken equal to 1 [35]. We also use shorthand notations $[S] = 2S + 1$ and $[\lambda]!! = (2\lambda + 1)!!$.

The reduced matrix elements are evaluated between the initial Ψ^J_{lS} and the final $\Psi^{J_f}_{l_f S'}$ state wave functions. The electric transition operator in the long-wavelength approximation reads as

$$M^E_{\lambda\mu} = e\sum_{j=1}^{A} Z_j r'^{\lambda}_j Y_{\lambda\mu}(\hat{r'}_j), \tag{10}$$

where $\vec{r'}_j = \vec{r}_j - \vec{R}_{\text{c.m.}}$ is the position of the jth particle in the center-of-mass system. Its reduced matrix elements can be evaluated as [2]

$$\begin{aligned}\langle \Psi^{J_f}_{l_f S'} \| M^E_\lambda \| \Psi^J_{lS}\rangle &= e\left[Z_1\left(\frac{A_2}{A}\right)^\lambda + Z_2\left(\frac{-A_1}{A}\right)^\lambda\right]\delta_{SS'} \\ &\times (-1)^{J+l+S}\left(\frac{[\lambda][l][J]}{4\pi}\right)^{1/2} C^{l_f 0}_{\lambda 0 l 0}\begin{Bmatrix} J & l & S \\ l_f & J_f & \lambda\end{Bmatrix} \\ &\times \int_0^\infty u_E^{(lSJ)}(r) r^\lambda u^{(l_f S J_f)}(r) dr, \end{aligned} \tag{11}$$

where $A_1,\ A_2$ are the mass numbers of the clusters in the entrance channel $A = A_1 + A_2$. The magnetic transition operator reads as [2]

$$\begin{aligned} M^M_{1\mu} &= \sqrt{\frac{3}{4\pi}}\sum_{j=1}^{A}\left[\mu_N \frac{Z_j}{A_j}\hat{l}_{j\mu} + 2\mu_j \hat{S}_{j\mu}\right] \\ &= \sqrt{\frac{3}{4\pi}}\left[\mu_N\left(\frac{A_2 Z_1}{AA_1} + \frac{A_1 Z_2}{AA_2}\right)\hat{l}_{r\mu} + 2(\mu_1 \hat{S}_{1\mu} + \mu_2 \hat{S}_{2\mu})\right], \end{aligned} \tag{12}$$

where μ_N is the nuclear magneton, μ_j is the magnetic moment, and $\hat{l}_{j\mu}$ ($\mu = -1, 0, +1$) is the projection of the orbital angular momentum of the jth particle. The projection of the orbital angular momentum of the relative motion is denoted as $\hat{l}_{r\mu}$. The magnetic $M1$ transition operator consists of the orbital and spin parts,

$$M^M_{1\mu} = \sqrt{\frac{3}{4\pi}}[M_1(l) + M_1(S)]. \tag{13}$$

The orbital part of the reduced matrix elements of the magnetic $M1$ transition operator reads as

$$\begin{aligned}\langle \Psi^{J_f}_{l_f S'} \| M_1(l) \| \Psi^J_{lS}\rangle &= \mu_N\left(\frac{A_2 Z_1}{AA_1} + \frac{A_1 Z_2}{AA_2}\right)\sqrt{l(l+1)[J][l]} \\ &\times (-1)^{\kappa_1}\begin{Bmatrix} l & S & J_f \\ J & 1 & l\end{Bmatrix}\delta_{l l_f}\delta_{SS'} I_{if}, \end{aligned} \tag{14}$$

where the exponential part of the phase factor $\kappa_1 = S + 1 + J + l$. The spin part of the magnetic $M1$ transition operator for the first particle (proton),

$$\begin{aligned}\langle \Psi^{J_f}_{l_f S'} \| M^M_1(S_1) \| \Psi^J_{lS}\rangle &= 2\mu_p(-1)^{\kappa_2}\sqrt{S_1(S_1+1)[S_1][S][S'][J]} \\ &\times \begin{Bmatrix} S_1 & S_2 & S \\ S' & 1 & S_1\end{Bmatrix}\begin{Bmatrix} S & l & J \\ J_f & 1 & S'\end{Bmatrix}\delta_{l l_f} I_{if}, \end{aligned} \tag{15}$$

with the exponential part of the phase factor $\kappa_2 = S_1 + S_2 + 2S + l + J_f$. In the above formula and everywhere we set $S_1 = S_p = 1/2,\ S_2 = S(^7\mathrm{Be}) = 3/2$ and $S' = S = 1$ due to the use of the single-channel approximation. The spin part of the reduced matrix elements of the $M1$ transition operator for the second particle (^{7}Be) reads as

$$\begin{aligned}\langle \Psi^{J_f}_{l_f S'} \| M^M_1(S_2) \| \Psi^J_{lS}\rangle &= 2\mu_{^7\mathrm{Be}}(-1)^{\kappa_3}\sqrt{S_2(S_2+1)[S_2][S][S'][J]} \\ &\times \begin{Bmatrix} S_2 & S_1 & S \\ S' & 1 & S_2\end{Bmatrix}\begin{Bmatrix} S & l & J \\ J_f & 1 & S'\end{Bmatrix}\delta_{l l_f} I_{if}, \end{aligned} \tag{16}$$

where $\kappa_3 = S_1 + S_2 + S + S' + l + J_f$ and the overlap integral is given as

$$I_{if} = \sqrt{\frac{3}{4\pi}}\int_0^\infty u_E^{(lSJ)}(r) u^{(l_f S' J_f)}(r) dr. \tag{17}$$

In the above equations the magnetic moments are taken as $\mu_p = 2.792\,847\mu_N$ and $\mu_{^7\mathrm{Be}} = -1.398\mu_N$ for the first and second particles, respectively.

Finally, the astrophysical S factor of the process is expressed in terms of the cross section with the help of the equation [43],

$$S(E) = E\sigma(E)\exp(2\pi\eta). \tag{18}$$

TABLE I. Values of the depth (V_0) and width (α_0) parameters of the original and modified $p - {}^7$Be potentials V_D and V_M in different partial waves.

$^{2S+1}L_J$	V_0 (MeV)	α_0 (fm^{-2})	E ^{8}B$_{\mathrm{FS}}$ (MeV)
$^3S_1$	−343.0	1.0	−110.13
$^3S_1$ (V_M)	−100.0	0.876	−2.42
$^3P_0$	−580.0	1.0	−102.25
$^3P_1$	−709.85	0.83	−205.38
$^3P_2$	−330.414634	0.375	−96.59
$^3S_2$ (V_M)	−300.5003	0.340	−87.86
$^3P_2$ (V_{M+})	−272.2387	0.307	−79.61
$^3P_2$ (V_{M-})	−333.8405	0.379	−95.59
$^3D_1$	−343.0	1.0	
$^3D_2$	−116.04	0.095	−20.45
$^3D_2$(V_M)	−193.0	0.15	−37.92
$^3D_3$	−343.0	1.0	
$^3F_3$	−104.555	0.055	−15.99

III. NUMERICAL RESULTS

A. Details of the calculations and interaction potentials

The Schrödinger equation in the entrance and exit channels is solved with the two-body $p - {}^7$Be central potentials of the Gaussian form [21] as defined in Eq. (7) with the corresponding pointlike Coulomb part. For consistency we use the same model parameters as in the aforementioned paper, i.e. $\hbar^2/2$ (amu) $= 20.7343$ MeV fm^2, $m_p = A_1$ amu $= 1.007\,276\,4669$ amu, $m_{^7\mathrm{Be}} = A_2$ amu $= 7.014\,735$ amu.

The scattering wave-function $u_E(r)$ of the relative motion is obtained by solving the Schrödinger equation using the Numerov method with an appropriate potential subject to the boundary condition specified in Eq. (6).

The depth V_0 and width α_0 of the $p - {}^7$Be potentials are given in Table I. We use four parameter sets for the original potential V_D from Ref. [21] and the modified potentials

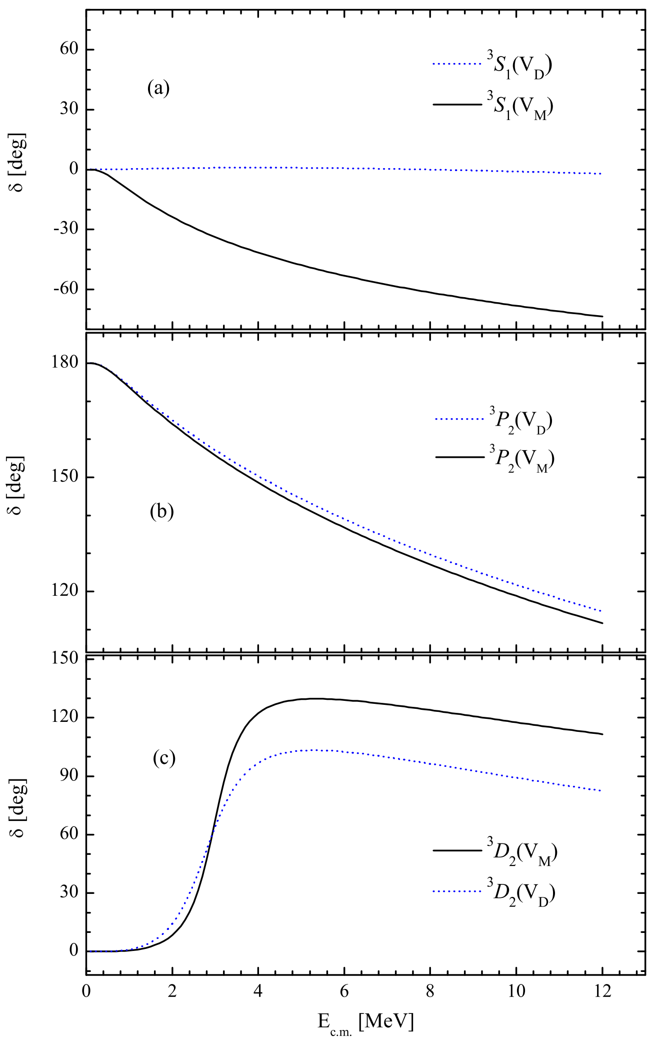

FIG. 1. Phase shifts in the (a) $^3S_1$, (b) $^3P_2$, and (c) $^3D_2$ partial waves of the $p-{}^7$Be scattering state with potentials V_D and V_M.

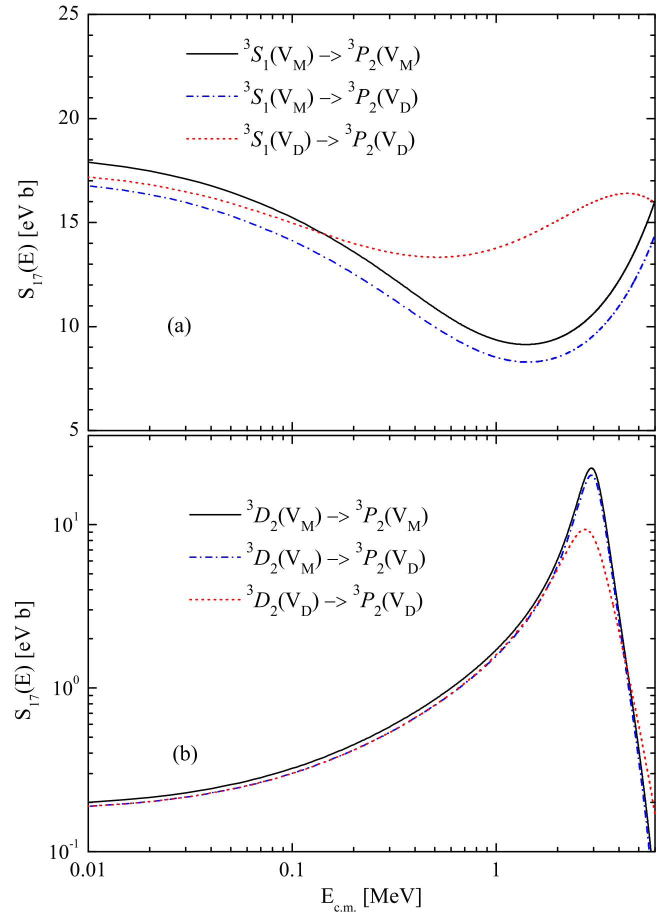

FIG. 2. Astrophysical S factors for the $^7\mathrm{Be}(p,\gamma)\,^8\mathrm{B}$ synthesis reaction due to the $E1$ transitions (a) $^3S_1 \to {}^3P_2$ and (b) $^3D_2 \to {}^3P_2$ estimated within the potential models V_D and V_M and their combination.

V_M, V_{M+}, and V_{M-}, respectively. The potentials V_D and V_M differ from each other only in the $^3S_1$, $^3P_2$, and $^3D_2$ partial waves, whereas potential models V_{M+} and V_{M-} differ from V_M only in the $^3P_2$ bound channel. The last column of the table contains energies of the forbidden states in the $^3S_1$, $^3P_1$, $^3P_2$, $^3P_3$, $^3D_2$ partial waves. The parameters of the modified V_M potential are fitted to reproduce the scattering length a_{01} in the $^3S_1$ partial wave, binding energy of the $^8\mathrm{B}(2^+,1)$ ground state and the experimental astrophysical S factor at the Gamow energy in the $^3P_2$ partial wave, and the experimental astrophysical S factor around the $^3D_2$ resonance.

First we examine how the scattering length a_{01} is described with the original V_D potential in the $^3S_1$ wave. As discussed in the Introduction, the most realistic experimental data $a_{01}^{\mathrm{exp}} = 17.34^{+1.11}_{-1.33}$ fm [38] for the spin = 1 channel should be reproduced by the $p-{}^7$Be potential. However, the original V_D potential yields an estimate of $a_{01}^{\mathrm{th}} = -0.26$ fm, which does not reproduce even the sign of the data. In Table I we present the fitted parameters of the new modified potential V_M in the $^3S_1$ partial wave which yields an estimate of $a_{01}^{\mathrm{th}} = 17.34$ fm for the scattering length. The parameters of the modified potentials V_M, V_{M+}, V_{M-} in the $^3P_2$ bound channel are adjusted according to two conditions. The first condition for the potential is the binding energy $E_b = 0.1375$ MeV of the $^8\mathrm{B}(2^+,1)$ ground state. The second condition comes from Eq. (2). It represents the experimental value of the astrophysical S factor at the Gamow solar energy. The potential V_M reproduces the central experimental value, whereas the potential models V_{M+} and V_{M-} reproduce the upper and lower boundaries of the astrophysical S factor at the Gamow energy, respectively. The last condition could as well be replaced by the relation,

$$S_s(0)/C^2 \approx 35.6(1-0.0014a_{01})\ \mathrm{eV\,b\,fm} \approx 34.74\ \mathrm{eV\,b\,fm}, \tag{19}$$

from Ref. [37], where a_{01} is in femtometers. This relationship connects the scattering length with the ANC and the astrophysical S factor at zero energy due to the transition from the initial S scattering wave. In other words, the above two conditions from Eqs. (2) and (19) should be equivalent. Since Eq. (19) needs an extrapolated value of the astrophysical S factor at $E=0$, its uncertainty is quite large. This is why we use Eq. (2) to define the potential parameters in the $^3P_2$

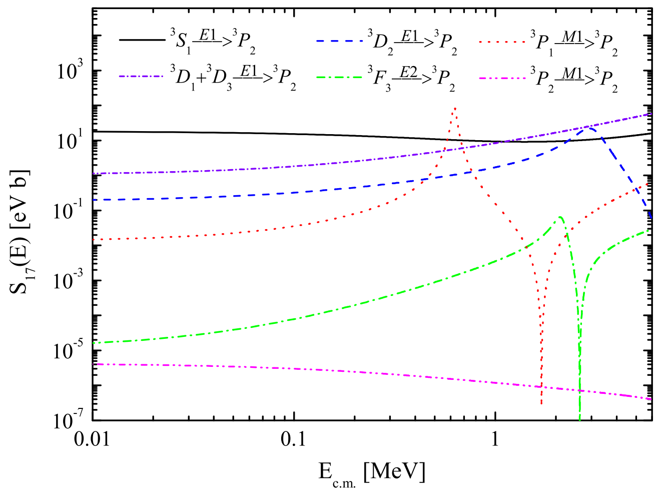

FIG. 3. The partial $E1$, $E2$, and $M1$ components of the astrophysical S factor for the ^{7}Be(p,γ) ^{8}B capture process within the V_M potential model.

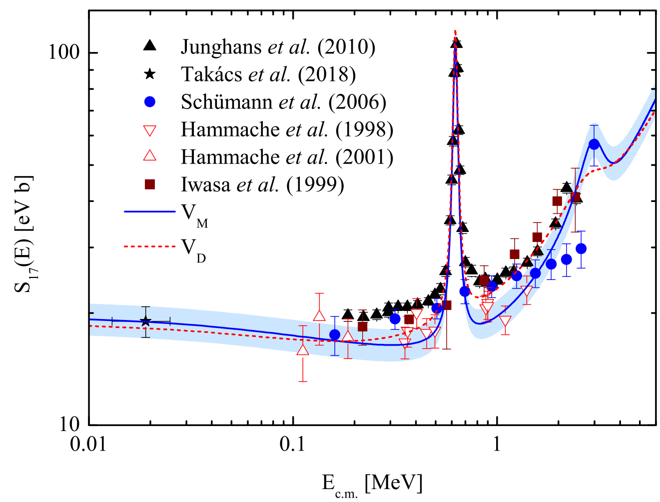

FIG. 4. Astrophysical S factor for the ^{7}Be(p,γ) ^{8}B synthesis reaction within the potential models V_D and V_M in comparison with available experimental data. The shaded area represents the uncertainty corresponding to the potential model V_M.

partial wave. Then consistency of the new potential with the relation in Eq. (19) will be examined. The original V_D and the modified V_M, V_{M+}, V_{M-} potentials yield values $C^2 = 0.496$, $C^2 = 0.538$, $C^2 = 0.590$, and $C^2 = 0.488$ fm^{-1}, respectively, for the ANC of the bound $^3P_2$ state.

Finally, the parameters of the modified potential in the partial $^3D_2$ wave are chosen to reproduce the astrophysical S factor in the second resonance region around $E = 3$ MeV.

In Fig. 1 we show the description of the phase shifts in the $^3S_1$, $^3P_2$, and $^3D_2$ partial waves. As can be seen from the figure, the potentials V_D and V_M yield a similar phase-shift description in the partial waves $^3P_2$ and $^3D_2$ but display significantly different descriptions in the partial $^3S_1$ wave channel.

B. The astrophysical *S* factor and the reaction rates of the ^{7}Be(p,γ) ^{8}B capture process

The astrophysical S factor and reaction rates of the ^{7}Be(p,γ) ^{8}B direct radiative-capture process presented below are calculated with the potentials V_D and V_M. The partial astrophysical S factors estimated with the above potential models and their combination for the initial $^3S_1$ channel are presented in Fig. 2 [panel (a)]. As can be seen, the potential model V_M yields results quite different from the V_D model ones for both absolute values and energy dependence of the S factor. This is, first, due to the fact that these models yield different values for the scattering length a_{01} and, second, due to the relation between the astrophysical S factor and the scattering length a_{01} given in Eq. (19). On the other hand, the value of $S_s(0.6\ \text{keV})/\text{C}^2 = 35.18$ eV b fm, calculated for the $^3S_1(V_M) \to {}^3P_2(V_D)$ transition with a combined potential model is larger than the value of 34.74 eV b fm from Eq. (19). The corresponding estimate for the $^3S_1(V_M) \to {}^3P_2(V_M)$ transition at the energy $E = 0.6$ keV is about 34.57 eV b fm, which is more consistent with the underlying theory [37].

In panel (b) of Fig. 2 we show the partial astrophysical S factors estimated for the initial $^3D_2$ resonance channel. Here the parameters of the model V_M have been adjusted to reproduce the experimental astrophysical S factor around the resonance energy. Below we see that this is possible.

Figure 3 compares the partial astrophysical S factors for different initial scattering channels obtained within the potential model V_M. One can see that the most important contribution at low energies comes from the initial $^3S_1$ channel due to the electric $E1$ transition. The $E1$ transitions from the initial $^3D_1$, $^3D_2$, and $^3D_3$ scattering channels altogether yield a contribution that is less than the contribution from the main $^3S_1$ channel by an order of magnitude at low energies. However, they become comparable at energies beyond the resonance region. The partial $M1$ transition from the initial $^3P_1$ scattering wave and $E1$ transition from the $^3D_2$ wave are

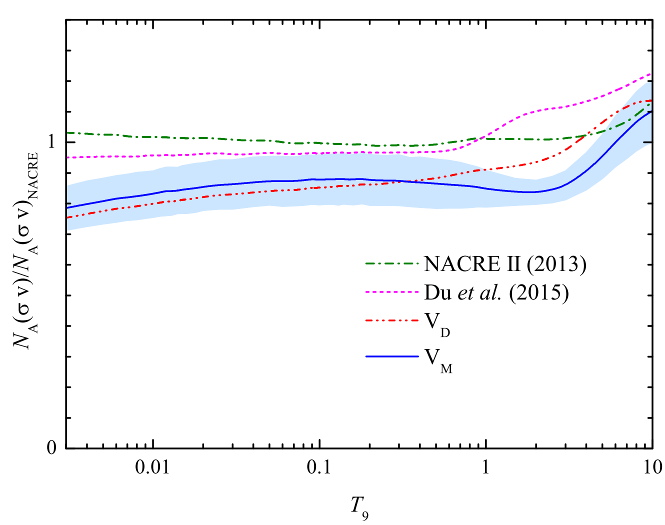

FIG. 5. Reaction rates of the direct $p + {}^7\text{Be} \to {}^8\text{B} + \gamma$ capture process within the V_D and V_M potential models normalized to the experimental data by the NACRE Collaboration [2]. The shaded area represents the uncertainty corresponding to the potential model V_M.

TABLE II. Theoretical estimations of the direct $^7\mathrm{Be}(p,\gamma)\,^8\mathrm{B}$ capture reaction rate in the temperature interval 10^6 K $\leqslant T \leqslant 10^{10}$ K ($0.001 \leqslant T_9 \leqslant 10$).

T_9	E_0 (MeV)	ΔE_0 (MeV)	$N_A(\sigma v)$ (cm^{3}mol^{-1}s^{-1})			
			V_D	V_M	V_{M+}	V_{M-}
0.001	0.003	0.001	4.99×10^{-38}	5.19×10^{-38}	5.67×10^{-38}	4.71×10^{-38}
0.002	0.005	0.002	5.19×10^{-29}	5.41×10^{-29}	5.91×10^{-29}	4.91×10^{-29}
0.003	0.006	0.003	1.21×10^{-24}	1.26×10^{-24}	1.37×10^{-24}	1.14×10^{-24}
0.004	0.007	0.004	6.77×10^{-22}	7.05×10^{-22}	7.71×10^{-22}	6.40×10^{-22}
0.005	0.009	0.004	6.07×10^{-20}	6.32×10^{-20}	6.91×10^{-20}	5.74×10^{-20}
0.006	0.010	0.005	1.87×10^{-18}	1.94×10^{-18}	2.12×10^{-18}	1.76×10^{-18}
0.007	0.011	0.006	2.87×10^{-17}	2.99×10^{-17}	3.26×10^{-17}	2.71×10^{-17}
0.008	0.012	0.007	2.72×10^{-16}	2.84×10^{-16}	3.10×10^{-16}	2.57×10^{-16}
0.009	0.013	0.007	1.82×10^{-15}	1.90×10^{-15}	2.07×10^{-15}	1.72×10^{-15}
0.010	0.014	0.008	9.35×10^{-15}	9.74×10^{-15}	1.06×10^{-14}	8.83×10^{-15}
0.011	0.015	0.009	3.90×10^{-14}	4.06×10^{-14}	4.44×10^{-14}	3.69×10^{-14}
0.012	0.015	0.009	1.38×10^{-13}	1.44×10^{-13}	1.57×10^{-13}	1.30×10^{-13}
0.013	0.016	0.010	4.27×10^{-13}	4.45×10^{-13}	4.86×10^{-13}	4.03×10^{-13}
0.014	0.017	0.010	1.18×10^{-12}	1.23×10^{-12}	1.34×10^{-12}	1.12×10^{-12}
0.015	0.018	0.011	2.97×10^{-11}	3.10×10^{-12}	3.38×10^{-12}	2.81×10^{-12}
0.016	0.019	0.012	6.92×10^{-12}	7.20×10^{-12}	7.87×10^{-12}	6.53×10^{-12}
0.018	0.020	0.013	3.07×10^{-11}	3.20×10^{-11}	3.50×10^{-11}	2.90×10^{-11}
0.020	0.022	0.014	1.11×10^{-10}	1.15×10^{-10}	1.26×10^{-10}	1.05×10^{-10}
0.025	0.025	0.017	1.44×10^{-9}	1.50×10^{-9}	1.64×10^{-9}	1.36×10^{-9}
0.030	0.028	0.020	1.01×10^{-8}	1.05×10^{-8}	1.15×10^{-8}	9.54×10^{-9}
0.040	0.034	0.025	1.72×10^{-7}	1.78×10^{-7}	1.95×10^{-7}	1.62×10^{-7}
0.050	0.040	0.030	1.27×10^{-6}	1.32×10^{-6}	1.44×10^{-6}	1.20×10^{-6}
0.060	0.045	0.035	5.81×10^{-6}	6.02×10^{-6}	6.58×10^{-6}	5.46×10^{-6}
0.070	0.050	0.040	1.95×10^{-5}	2.02×10^{-5}	2.20×10^{-5}	1.83×10^{-5}
0.080	0.055	0.045	5.27×10^{-5}	5.45×10^{-5}	5.95×10^{-5}	4.94×10^{-5}
0.090	0.059	0.049	1.22×10^{-4}	1.26×10^{-4}	1.37×10^{-4}	1.14×10^{-4}
0.100	0.063	0.054	2.50×10^{-4}	2.58×10^{-4}	2.82×10^{-4}	2.34×10^{-4}
0.110	0.068	0.058	4.69×10^{-4}	4.83×10^{-4}	5.27×10^{-4}	4.38×10^{-4}
0.120	0.072	0.063	8.15×10^{-4}	8.39×10^{-4}	9.17×10^{-4}	7.61×10^{-4}
0.130	0.076	0.067	1.34×10^{-3}	1.37×10^{-3}	1.50×10^{-3}	1.24×10^{-3}
0.140	0.079	0.072	2.09×10^{-3}	2.14×10^{-3}	2.34×10^{-3}	1.94×10^{-3}
0.150	0.083	0.076	3.12×10^{-3}	3.20×10^{-3}	3.49×10^{-3}	2.90×10^{-3}
0.160	0.087	0.080	4.51×10^{-3}	4.61×10^{-3}	5.04×10^{-3}	4.18×10^{-3}
0.180	0.094	0.088	8.63×10^{-3}	8.81×10^{-3}	9.63×10^{-3}	7.99×10^{-3}
0.200	0.101	0.096	1.51×10^{-2}	1.53×10^{-2}	1.68×10^{-2}	1.39×10^{-2}
0.250	0.117	0.116	4.58×10^{-2}	4.63×10^{-2}	5.06×10^{-2}	4.20×10^{-2}
0.300	0.132	0.135	1.06×10^{-1}	1.07×10^{-1}	1.17×10^{-1}	9.68×10^{-2}
0.350	0.146	0.153	2.07×10^{-1}	2.07×10^{-1}	2.26×10^{-1}	1.88×10^{-1}
0.400	0.160	0.172	3.59×10^{-1}	3.57×10^{-1}	3.90×10^{-1}	3.23×10^{-1}
0.500	0.186	0.207	8.53×10^{-1}	8.35×10^{-1}	9.13×10^{-1}	7.58×10^{-1}
0.600	0.210	0.240	1.66×10^{0}	1.60×10^{0}	1.75×10^{0}	1.46×10^{0}
0.700	0.232	0.273	2.85×10^{0}	2.72×10^{0}	2.96×10^{0}	2.49×10^{0}
0.800	0.254	0.306	4.50×10^{0}	4.27×10^{0}	4.61×10^{0}	3.92×10^{0}
0.900	0.275	0.337	6.69×10^{0}	6.28×10^{0}	6.76×10^{0}	5.81×10^{0}
1.000	0.295	0.368	9.46×10^{0}	8.82×10^{0}	9.44×10^{0}	8.20×10^{0}
1.500	0.386	0.516	3.18×10^{1}	2.89×10^{1}	3.04×10^{1}	2.74×10^{1}
2.000	0.468	0.656	6.45×10^{1}	5.78×10^{1}	6.05×10^{1}	5.51×10^{1}
2.500	0.543	0.790	1.03×10^{2}	9.13×10^{1}	9.59×10^{1}	8.67×10^{1}
3.000	0.613	0.919	1.45×10^{2}	1.28×10^{2}	1.35×10^{2}	1.21×10^{2}
4.000	0.743	1.168	2.38×10^{2}	2.10×10^{2}	2.24×10^{2}	1.96×10^{2}
5.000	0.862	1.407	3.41×10^{2}	3.05×10^{2}	3.28×10^{2}	2.82×10^{2}
6.000	0.973	1.638	4.53×10^{2}	4.12×10^{2}	4.47×10^{2}	3.79×10^{2}
7.000	1.078	1.863	5.71×10^{2}	5.30×10^{2}	5.76×10^{2}	4.84×10^{2}
8.000	1.179	2.082	6.93×10^{2}	6.55×10^{2}	7.14×10^{2}	5.96×10^{2}
9.000	1.275	2.297	8.18×10^{2}	7.84×10^{2}	8.57×10^{2}	7.13×10^{2}
10.00	1.368	2.507	9.45×10^{2}	9.18×10^{2}	1.00×10^{3}	8.33×10^{2}

responsible for the first and second resonances at energies 0.633 and 2.988 MeV, respectively.

In Fig. 4 we present the total astrophysical S factor of the ^{7}Be(p,γ) ^{8}B process obtained within the potential models V_D and V_M. The uncertainty in the results with the V_M model shown as a shaded area originates from the upper and lower boundaries of Eq. (2). They are obtained with the potentials V_{M+} and V_{M-}, respectively.

As can be seen from the figure, the results for the potential model V_M are mostly consistent with the two data sets of Hammache *et al.* [10,11]. Other measurements [12,14,17,39] show higher values in the vicinity of the resonance.

A behavior of the astrophysical S factor near zero energy is more complex. Our estimates within the V_M potential model are $S_{17}(1\text{ keV}) = 19.64$ and $S_{17}(0.6\text{ keV}) = 20.07$ eV b. An extrapolation to the zero energy with the help of the ANC method [44] yields

$$S_{17}(0) \approx 20.51\text{ eV b}. \tag{20}$$

The corresponding extrapolation for the potential models V_{M+} and V_{M-} yields upper and lower boundary values,

$$S_{17}(0) \approx 22.53\text{ eV b}, \tag{21}$$

$$S_{17}(0) \approx 18.66\text{ eV b}. \tag{22}$$

Our estimates are slightly lower than the SF II estimate [3] quoted in Eq. (1).

Finally, estimated reaction rates within the models V_D and V_M are presented in Table II and Fig. 5. The last two columns of Table II present the upper and lower boundaries for the reaction rate, obtained with the potential V_M. In the second and third columns of the table, "the most effective" energy E_0 and the width of the Gamow window ΔE_0 are given [2]. One can note that our theoretical results are substantially lower than the estimates of the NACRE II Collaboration [45] and Du *et al.* [46].

IV. CONCLUSIONS

The astrophysical ^{7}Be(p,γ) ^{8}B direct capture process has been studied within the two-body potential model using the single-channel approximation. The modified potential is constructed to reproduce the new experimental value of the S-wave-scattering length and the known astrophysical S factor at the Gamow energy, extracted from the solar neutrino flux. The modified potential is consistent with the theory of Baye [36] which connects the S-wave-scattering length with the astrophysical S factor at zero energy divided by the square of ANC.

The results obtained for the astrophysical S factor within the modified potential approach are in accordance with the data of Hammache *et al.* in contrast to those obtained using the original potential by Dubovichenko *et al.* [21]. The value of the astrophysical S factor extrapolated to zero energy is found to be $S_{17}(0) \approx 20.51^{+2.02}_{-1.85}$ eV b which is consistent with the SF II estimates [3]. Although its uncertainty is marginally different from the total uncertainty of 2.1 eV b of the Solar Fusion II model, it is somewhat larger than the theoretical uncertainty of 1.4 eV b. Another important result is that the calculated reaction rates are lower than the results of the NACRE II Collaboration [45].

ACKNOWLEDGMENTS

We thank D. Baye for stimulating discussions of the problem. A.S.K. acknowledges the support from the Australian Research Council. L.D.B. acknowledges support by the Russian Foundation for Basic Research Grant No. 19-02-00014.

[1] C. E. Rolfs and W. S. Rodney, *Cauldrons in the Cosmos* (University of Chicago Press, Chicago, 1988).
[2] C. Angulo *et al.* (NACRE Collaboration), Nucl. Phys. A **656**, 3 (1999).
[3] E. G. Adelberger *et al.*, Rev. Mod. Phys. **83**, 195 (2011).
[4] B. D. Fields, Ann. Rev. Nucl. Part. Sci. **61**, 47 (2011).
[5] S. N. Ahmed *et al.* (SNO Collaboration), Phys. Rev. Lett. **92**, 181301 (2004).
[6] B. W. Filippone, A. J. Elwyn, C. N. Davids, and D. D. Koetke, Phys. Rev. Lett. **50**, 412 (1983).
[7] T. Motobayashi, N. Iwasa, Y. Ando *et al.*, Phys. Rev. Lett. **73**, 2680 (1994).
[8] L. T. Baby *et al.*, Phys. Rev. Lett. **90**, 022501 (2003)
[9] A. R. Junghans *et al.*, Phys. Rev. C **68**, 065803 (2003).
[10] F. Hammache *et al.*, Phys. Rev. Lett. **80**, 928 (1998).
[11] F. Hammache *et al.*, Phys. Rev. Lett. **86**, 3985 (2001).
[12] A. R. Junghans, K. A. Snover, E. C. Mohrmann, E. G. Adelberger, and L. Buchmann, Phys. Rev. C **81**, 012801(R) (2010).
[13] G. Baur, C. A. Bertulani, and H. Rebel, Nucl. Phys. A **458**, 188 (1986).
[14] N. Iwasa *et al.*, Phys. Rev. Lett. **83**, 2910 (1999).
[15] B. Davids *et al.*, Phys. Rev. Lett. **86**, 2750 (2001).
[16] F. Schümann *et al.*, Phys. Rev. Lett. **90**, 232501 (2003).
[17] F. Schümann *et al.*, Phys. Rev. C **73**, 015806 (2006).
[18] R. G. H. Robertson, Phys. Rev. C **7**, 543 (1973).
[19] S. Typel, H. H. Wolter, and G. Baur, Nucl. Phys. A **613**, 147 (1997).
[20] B. Davids and S. Typel, Phys. Rev. C **68**, 045802 (2003).
[21] S. B. Dubovichenko, N. A. Burkova, A. V. Dzhazairov-Kakhramanov, and A. S. Tkachenko, Nucl. Phys. A **983**, 175 (2019).
[22] F. C. Barker, Nucl. Phys. A **588**, 693 (1995).
[23] P. Descouvemont and D. Baye, Nucl. Phys. A **567**, 341 (1994).
[24] A. Csoto, K. Langanke, S. E. Koonin, and T. D. Shoppa, Phys. Rev. C **52**, 1130 (1995).
[25] P. Descouvemont, Phys. Rev. C **70**, 065802 (2004).
[26] L. V. Grigorenko, B. V. Danilin, V. D. Efros, N. B. Shulgina, and M. V. Zhukov, Phys. Rev. C **57**, R2099(R) (1998).
[27] P. Navratil, C. A. Bertulani, and E. Caurier, Phys. Rev. C **73**, 065801 (2006).
[28] P. Navratil, R. Roth, and S. Quaglioni, Phys. Lett. B **704**, 379 (2011).
[29] S. S. Chandel, S. K. Dhiman, and R. Shyam, Phys. Rev. C **68**, 054320 (2003).

[30] X. Zhang, K. M. Nollett, and D. R. Phillips, Phys. Lett. B **751**, 535 (2015).
[31] A. Azhari, V. Burjan, F. Carstoiu, H. Dejbakhsh, C. A. Gagliardi, V. Kroha, A. M. Mukhamedzhanov, L. Trache, and R. E. Tribble, Phys. Rev. Lett. **82**, 3960 (1999).
[32] O. R. Tojiboev, R. Yarmukhamedov, S. V. Artemov, and S. B. Sakuta, Phys. Rev. C **94**, 054616 (2016).
[33] L. Trache, A. Azhari, F. Carstoiu, H. L. Clark, C. A. Gagliardi, Y.-W. Lui, A. M. Mukhamedzhanov, X. Tang, N. Timofeyuk, and R. E. Tribble, Phys. Rev. C **67**, 062801(R) (2003).
[34] A. M. Mukhamedzhanov and N. K. Timofeyuk, Yad. Fiz. **51**, 679 (1990) [Sov. J. Nucl. Phys. **51**, 431 (1990)].
[35] A. M. Mukhamedzhanov, Shubhchintak, and C. A. Bertulani, Phys. Rev. C **93**, 045805 (2016).
[36] D. Baye, Phys. Rev. C **62**, 065803 (2000).
[37] D. Baye and E. Brainis, Phys. Rev. C **61**, 025801 (2000).
[38] S. N. Paneru, C. R. Brune, R. Giri, R. J. Livesay, U. Greife, J. C. Blackmon, D. W. Bardayan, K. A. Chipps, B. Davids, D. S. Connolly, K. Y. Chae, A. E. Champagne, C. Deibel, K. L. Jones, M. S. Johnson, R. L. Kozub, Z. Ma, C. D. Nesaraja, S. D. Pain, F. Sarazin *et al.*, Phys. Rev. C **99**, 045807 (2019).
[39] M. P. Takács, D. Bemmerer, A. R. Junghans, and K. Zuber, Nucl. Phys. **A970**, 78 (2018).
[40] E. M. Tursunov, S. A. Turakulov, and P. Descouvemont, Phys. At. Nucl. **78**, 193 (2015).
[41] E. M. Tursunov, S. A. Turakulov, and A. S. Kadyrov, Phys. Rev. C **97**, 035802 (2018).
[42] E. M. Tursunov, S. A. Turakulov, and A. S. Kadyrov, Nucl. Phys. A **1006**, 122108 (2021).
[43] W. A. Fowler, G. R. Gaughlan, and B. A. Zimmerman, Annu. Rev. Astron. Astrophys. **13**, 69 (1975).
[44] G. G. Kiss *et al.*, Phys. Rev. C **104**, 015807 (2021).
[45] Y. Xu *et al.* (NACRE II Collaboration), Nucl. Phys. A **918**, 61 (2013).
[46] X. C. Du, B. Guo, Z. H. Li, D. Y. Pang, E. T. Li, and W. P. Liu, Sci. China Phys., Mech. Astron. **58**, 1 (2015).